A comparison between GATE4 results and MCNP4B published data for internal radiation dosimetry

A. A. Parach; H. Rajabi
Dept. of Medical Physics, School of Medical Sciences, Tarbiat Modares University, Tehran, Iran

Keywords
Monte Carlo, radionuclide dosimetry, GATE, voxel phantom

Summary
Aim: GATE, has been designed as upper layer of the GEANT4 toolkit for nuclear medicine application including internal dosimetry. However, its results have not been fully compared to the well-developed codes and anthropomorphic voxel phantoms have never been used with GATE/GEANT for internal dosimetry. The aim of present study was to compare the internal dose calculated by GATE/GEANT with the MCNP4B published data. Methods: The Zubal phantom was used to model a typical adult male. Activity was assumed uniformly distributed in liver, kidneys, lungs, spleen, pancreas and adrenals. GATE/GEANT Monte Carlo package was used for estimation of doses in the phantom. Simulations were performed for photon energy of 0.01–1 MeV and mono-energetic electrons of 935 keV. Specific absorbed fractions for photons and S-factors for electrons were calculated. Results: On average, GATE/GEANT produces higher photon SAF (Specific Absorbed Fraction) values (+2.7%) for self-absorption and lower values (-2.9%) for cross-absorption. The difference was higher for paired organs particularly lungs. Moreover the photon SAF values for lungs as source organ at the energy of 200 and 500 keV was considerably higher with MCNP4B compared to GATE. Conclusion: Despite of differences between the GATE4 and MCNP4B, the results can be considered ensuring. This may be considered as validation of GATE/GEANT as a proprietary code in nuclear medicine for radionuclide dosimetry applications.

Schlüsselwörter
Monte Carlo, Radionuklid-Dosimetrie, GATE, Voxel-Phantom

Zusammenfassung
Ziel: GATE wurde als oberste Schicht des GEANT4-Toolkits für nuklearmedizinische Anwendungen einschließlich interner Dosimetrie entwickelt. Jedoch wurden seine Ergebnisse nicht vollständig mit den ausgereiften Codes verglichen und es wurden noch nie anthropomorphe Voxel-Phantome mit dem GATE/GEANT zur internen Dosimetrie eingesetzt. In dieser Studie sollte die mit dem GATE/GEANT berechnete interne Dosis mit den für MCNP4P publizierten Daten verglichen werden. Methoden: Das Zubal-Phantom diente als Modell eines typischen männlichen Erwachsenen. Wir nahmen an, dass sich die Aktivität gleichmäßig in Leber, Nieren, Lungen, Milz, Pankreas und Nebennieren verteilt. Zur Dosisschätzung in dem Phantom wurde das GATE/GEANT-Monte-Carlo-Paket verwendet. Die Simulationen wurden für eine Photonenenergie von 0,01–1 MeV und monoenergetische Elektronen von 935 KeV durchgeführt. Es wurden die spezifischen absorbierten Fraktionen für Protonen und die S-Faktoren für Elektronen berechnet. Ergebnisse: Im Durchschnitt ergibt das GATE/GEANT höhere SAF (spezifische absorbierte Fraktion) Werte (+ 2,7%) für Selbstabsorption und niedrigere Werte (–2,9%) für Kreuzabsorption. Bei paarig angelegten Organen, insbesondere den Lungen, war der Unterschied größer. Darüber hinaus waren die Photonen-SAF-Werte für die Lungen als Ursprungsorgan bei einer Energie von 200 und 500 KeV mit MCNP4B deutlich höher als mit GATE. Schlussfolgerung: Trotz der Unterschiede zwischen GATE4 und MCNP4B halten wir die Ergebnisse für ermutigend. Die Studie kann als Validierung des GATE/GEANT-Systems als urheberrechtlich geschützter Code für die Radionuklid-Dosimetrie bei nuklearmedizinischen Anwendungen gelten.

Correspondence to:
Hossein Rajabi
Dept. of Medical Physics, Faculty of Medical Sciences
Tarbiat Modares University, Tehran-Iran
P.O. Box 14115–331, Tehran, Iran
Tel. +98/21/82 88 38 94
E-mail: hRajabi@modares.ac.ir

Ein Vergleich zwischen GATE4-Ergebnissen und publizierten Daten zu MCNP4B für die interne Strahlungsdosimetrie
Nuklearmedizin 2011; 50: 122–133
doi:10.3413/Nukmed-0363-10-10
received: October 27, 2010
accepted in revised form: January 13, 2011
prepublished online: February 22, 2011

To permit efficient delivery of high amounts of radiation dose to tumours while limiting radiation dose to critical organs, dosimetry calculations have to be performed (15).

> Patient-specific dosimetry is essential for prediction of the tumour response and also evaluation of the absorbed dose for therapeutic applications (16).

Theoretically Monte Carlo simulation is the most suitable method for patient-specific dose assessment (32). Anatomical information and attenuation coefficients of the tissues may be obtained using computed tomography images. Distribution of radiopharmaceutical within the patient body may be determined using SPECT or PET images. With this information avail-

able, it is possible to estimate the dose distribution within the patient's body at voxel level (14) by the use of Monte Carlo simulation or other personalized 3-dimentional codes such as

- Oedipe (12),
- 3D-ID (24),
- 3D-RD (20).

Current imaging technology provides sufficient accuracy at sub-millimeter resolution for anatomical and attenuation properties of the tissues. However, determining the activity distribution with sufficient accuracy is not yet achievable. Current nuclear medicine imaging systems suffer from poor temporal and energy resolution that is reflected as poor spatial resolution and poor efficiency in rejection of scatter photons. Photon attenuation further degrades the quality of images. Such effects have a large impact on quantitative accuracy of images and all have to be corrected for, in order to obtain optimal images (37). Fortunately, there has been considerable progress in correction for the image degrading factors that eventually will lead to provide quantitative images suitable for accurate dose estimation (3, 26, 37).

With adequate accuracy of the input data, the accuracy of dose estimation will ultimately depend upon the accuracy of the Monte Carlo code used for simulation. However, Monte Carlo codes are different in the method of random number generation, table of materials cross sections, approximations used in formulation of physical models and the strategy for the particle tracking (1, 7). Moreover, some limits are usually imposed to the particle tracking process depending on the special purpose the code is designed for (1). We have also to consider the possibility of bugs in any type of software.

Principally, a newly developed code should be validated against experimental data. However, this is not possible for internal dosimetry, because direct measurement of the dose to the tissues from internally administrated radioisotopes is not possible. In practice, some simple forms of physical phantom are used for validation of the Monte Carlo codes. However, phantom studies are limited to measurement of average dose in a few locations inside the phantoms. Physical structure and materials of the phantoms are extremely simple compared to the human anatomy and detector used for measurement further deteriorates the situation. Most of the radiation detectors are not tissue equivalent, while this is not of major concern for the megavoltage photons, problems can arise at low- to medium-energy photons that we mostly encounter in nuclear medicine (25). Moreover, dose measurement using detectors such as ionizing chamber or TLD (thermoluminescent dosimeter) is generally based on the induction of electrical charge or electron transition in the sensitive materials of the detector not the energy delivered to it. Though charge production and electron transition are related to the absorbed energy, they are not the same and calibration is required to calculate the dose. This may be problematic in determining the absolute dose, depending on chemical structure of the detector material. This fact may be acknowledge considering the strong dependency of photoelectric effect on the effective atomic number of the material in which the energy is deposited (25).

Another problem in experimental validation of Monte Carlo codes with experimental data is the type and the energy of the radiation emitting from the radioisotopes. The material used for detection of â-particles and ã-photons are different and are sensitive within a limited range of energy whereas, many radioisotopes produce both types of radiation at a wide range of energy. Even using the proper technique and instruments, the accuracy of measurement is limited to ±5% at the best situation (35). We have also to consider that there is always considerable error in measuring activity of the radioisotopes used for the experiments. Therefore, experimental studies do not provide the required accuracy and precision for the absolute validation of Monte Carlo codes for internal dosimetry. Validation of new codes for the internal dosimetry is ultimately restricted to comparison with well-developed and thoroughly validated codes.

A number of Monte Carlo codes are now available for dosimetry applications. MCNP (6) and EGS (23) and GEANT4 (17, 31) are general purpose codes developed to simulate interaction of photons and electrons with materials that can be used for internal dose assessment. Radiotherapy dedicated codes are also available to determine the dose from external sources of radiation to the patient (39). GATE/GEANT package is the most recently developed Monte Carlo code with the ambition to become the gold standard code in nuclear medicine (33). GATE/GEANT that has been developed as the upper layer of GEANT4 toolkit and is practically the only nuclear medicine dedicated code with options for different types of imaging and determining the dose distribution inside the body.

GATE/GEANT has certain attractive features for internal dosimetry application (39). It includes a very flexible simulation geometry input capable to accommodate a large variety of detector and source geometries. It also includes a user-friendly implemented voxelized source and a virtual clock to allow simulation of temporal phenomena such as source and detector movements and source decay. GATE/GEANT is very flexible for simulating complex detector geometries and experimental arrangements.

Although GEANT4 is an almost validated code (8, 17, 22, 31, 41), but it is itself a new code and less experienced compared to older code like MCNP and not properly validated for internal dosimetry. GATE/GENAT is partially validated for imaging applications (2, 10, 21, 36) and has been used for dosimetry applications (28, 38, 39) but not validated for nuclear medicine dosimetry. Moreover, results of this code have never been compared to the results obtained with older Monte Carlo packages like MCNP. General-purpose codes like MCNP and EGS have extensively been validated for different applications. Comparison to this codes may be considered as an essential step in validation of new codes like GATE/GEANT.

In this study, we calculated the organ doses using the Zubal voxel phantom (42) with GATE/GEANT for electron and photons of different energies and the results were compared to similar results obtained using MCNP4B and MCNPX Monte Carlo codes (12, 34, 40). We calculated the self-absorption and cross-irradiation of the organs for electron and photons in terms of S-factors and specific absorbed fractions (SAF) respectively.

energy (keV)	target organ	method	source organ					
			liver	kidneys	lungs	pancreas	spleen	adrenals
10	liver	GATE	4.94E-01	2.98E-03	1.11E-03	1.86E-04	0.00E+00	8.81E-03
		MCNP4B	4.91E-01	3.30E-03	1.19E-03	2.09E-04	0.00E+00	9.87E-03
	kidneys	GATE	2.99E-03	1.83E+00	0.00E+00	1.20E-02	5.56E-03	7.18E-02
		MCNP4B	3.25E-03	1.81E+00	0.00E+00	1.35E-02	6.18E-03	7.97E-02
	lungs	GATE	1.25E-03	0.00E+00	7.56E-01	0.00E+00	4.43E-03	1.69E-08
		MCNP4B	1.27E-03	0.00E+00	7.51E-01	0.00E+00	4.54E-03	0.00E+00
	pancreas	GATE	1.71E-04	1.20E-02	0.00E+00	1.69E+01	0.00E+00	3.38E-01
		MCNP4B	2.13E-04	1.40E-02	0.00E+00	1.66E+01	0.00E+00	3.71E-01
	spleen	GATE	0.00E+00	5.54E-03	3.95E-03	2.56E-08	2.55E+00	1.46E-07
		MCNP4B	0.00E+00	6.28E-03	4.06E-03	0.00E+00	2.53E+00	0.00E+00
	adrenals	GATE	8.74E-03	7.23E-02	0.00E+00	3.36E-01	0.00E+00	1.80E+02
		MCNP4B	9.11E-03	8.05E-02	0.00E+00	3.75E-01	0.00E+00	1.71E+02
15	liver	GATE	4.55E-01	9.52E-03	4.42E-03	3.37E-03	4.93E-07	2.29E-02
		MCNP4B	4.50E-01	1.03E-02	4.75E-03	3.83E-03	8.51E-07	2.47E-02
	kidneys	GATE	9.53E-03	1.56E+00	2.14E-05	3.61E-02	1.99E-02	1.80E-01
		MCNP4B	1.04E-02	1.52E+00	2.96E-05	3.92E-02	2.17E-02	1.92E-01
	lungs	GATE	5.03E-03	2.47E-05	6.05E-01	1.54E-05	1.31E-02	1.03E-04
		MCNP4B	5.31E-03	2.88E-05	5.94E-01	2.19E-05	1.37E-02	1.27E-04
	pancreas	GATE	3.39E-03	3.61E-02	1.22E-05	1.32E+01	3.28E-04	6.12E-01
		MCNP4B	3.65E-03	3.84E-02	1.58E-05	1.27E+01	4.17E-04	6.45E-01
	spleen	GATE	5.50E-07	1.99E-02	1.16E-02	3.24E-04	2.25E+00	7.47E-04
		MCNP4B	0.00E+00	2.18E-02	1.21E-02	3.98E-04	2.22E+00	9.34E-04
	adrenals	GATE	2.28E-02	1.80E-01	6.69E-05	6.10E-01	8.18E-04	1.06E+02
		MCNP4B	2.49E-02	1.94E-01	1.01E-04	6.49E-01	9.10E-04	9.57E+01
20	liver	GATE	3.97E-01	1.93E-02	1.05E-02	1.47E-02	5.10E-05	4.25E-02
		MCNP4B	3.91E-01	2.04E-02	1.11E-02	1.59E-02	5.81E-05	4.49E-02
	kidneys	GATE	1.93E-02	1.22E+00	4.53E-04	6.03E-02	4.34E-02	2.35E-01
		MCNP4B	2.03E-02	1.18E+00	5.48E-04	6.35E-02	4.60E-02	2.42E-01
	lungs	GATE	1.19E-02	5.18E-04	4.29E-01	7.18E-04	2.39E-02	1.68E-03
		MCNP4B	1.23E-02	5.55E-04	4.16E-01	8.21E-04	2.43E-02	1.81E-03
	pancreas	GATE	1.46E-02	6.05E-02	6.28E-04	9.09E+00	6.36E-03	6.75E-01
		MCNP4B	1.58E-02	6.33E-02	6.08E-04	8.58E+00	7.33E-03	6.91E-01
	spleen	GATE	4.98E-05	4.34E-02	2.12E-02	6.37E-03	1.82E+00	7.71E-03
		MCNP4B	5.72E-05	4.60E-02	2.18E-02	7.32E-03	1.77E+00	8.59E-03
	adrenals	GATE	4.30E-02	2.35E-01	1.44E-03	6.75E-01	7.87E-03	5.75E+01
		MCNP4B	4.37E-02	2.44E-01	1.15E-03	6.95E-01	6.11E-03	5.05E+01

Tab. 1
SAF values (kg^{-1}) for 10–50 keV photons derived with GATE 4.0.0 and MCNP4B (data derived from ref. 34, 40) using Zubal phantom

Tab. 1
Continued

energy (keV)	target organ	method	source organ					
			liver	kidneys	lungs	pancreas	spleen	adrenals
30	liver	GATE	2.74E-01	3.20E-02	1.82E-02	3.60E-02	1.36E-03	6.93E-02
		MCNP4B	2.67E-01	3.26E-02	1.85E-02	3.67E-02	1.36E-03	7.02E-02
	kidneys	GATE	3.21E-02	6.73E-01	3.31E-03	7.67E-02	6.68E-02	2.04E-01
		MCNP4B	3.25E-02	6.41E-01	3.40E-03	7.69E-02	6.77E-02	2.00E-01
	lungs	GATE	2.03E-02	3.66E-03	2.06E-01	7.01E-03	3.06E-02	9.45E-03
		MCNP4B	2.02E-02	3.63E-03	1.96E-01	7.02E-03	3.02E-02	9.26E-03
	pancreas	GATE	3.59E-02	7.68E-02	6.37E-03	4.15E+00	3.51E-02	5.11E-01
		MCNP4B	3.61E-02	7.81E-02	6.61E-03	3.84E+00	3.65E-02	5.06E-01
	spleen	GATE	1.35E-03	6.66E-02	2.75E-02	3.50E-02	1.04E+00	2.59E-02
		MCNP4B	1.37E-03	6.80E-02	2.74E-02	3.65E-02	1.00E+00	2.65E-02
	adrenals	GATE	6.87E-02	2.03E-01	8.60E-03	5.10E-01	2.61E-02	2.04E+01
		MCNP4B	6.40E-02	2.01E-01	8.72E-03	5.01E-01	2.63E-02	1.73E+01
50	liver	GATE	1.44E-01	3.02E-02	1.74E-02	3.84E-02	4.67E-03	6.18E-02
		MCNP4B	1.42E-01	3.00E-02	1.75E-02	3.80E-02	4.47E-03	6.09E-02
	kidneys	GATE	3.02E-02	2.82E-01	6.41E-03	6.20E-02	5.23E-02	1.20E-01
		MCNP4B	3.00E-02	2.71E-01	6.19E-03	6.04E-02	5.19E-02	1.15E-01
	lungs	GATE	1.87E-02	6.76E-03	8.43E-02	1.26E-02	2.34E-02	1.46E-02
		MCNP4B	1.84E-02	6.50E-03	8.03E-02	1.22E-02	2.30E-02	1.37E-02
	pancreas	GATE	3.85E-02	6.23E-02	1.19E-02	1.46E+00	4.59E-02	2.66E-01
		MCNP4B	3.79E-02	5.86E-02	1.16E-02	1.38E+00	4.56E-02	2.59E-01
	spleen	GATE	4.61E-03	5.21E-02	2.17E-02	4.51E-02	4.41E-01	3.07E-02
		MCNP4B	4.38E-03	5.18E-02	2.16E-02	4.56E-02	4.30E-01	2.99E-02
	adrenals	GATE	6.19E-02	1.19E-01	1.37E-02	2.66E-01	3.09E-02	6.02E+00
		MCNP4B	5.97E-02	1.18E-01	1.41E-02	2.59E-01	3.02E-02	5.35E+00

Material and methods

Phantom

The voxel-based anthropomorphic Zubal phantom was used to model a typical adult male (42). The phantom included head and body torso (no arms or legs) segmented into 56 different tissue types. The phantom consisted of 128×128×243 voxels of 4×4×4 mm dimensions. Six copies of the phantom were generated and the activity was distributed uniformly within the liver, kidneys, lungs, spleen, pancreas and the adrenal glands of the phantoms respectively. This geometry was exactly the same as the geometry used by Yoriyaz et al. and Chiavassa et al. (11, 40).

Monte Carlo simulation

GATE/GEANT Monte Carlo package (version 4.0.0) was used for estimation of dose to the organs of the phantoms (39). This version of GATE/GEANT was developed over GEANT4 version 4.9.1.p02. Photoelectric absorption, Compton interaction, Rayleigh scattering and characteristic X-ray production were considered for photon interactions. X-rays were tracked down to 1 keV, below that was assumed absorbed in the same voxel. Ionization, multiple scattering and bremsstrahlung were considered for electron interactions. The cutoff range applied on the secondary electrons was 1 mm. Each voxel in the phantoms was linked to the table describing the attenuation properties (composition and density) of the corresponding tissues (39). Simulations were performed for the photons of 10, 15, 20, 30, 50, 100, 200, 500, 1000 keV and the mono-energetic electrons of 935 keV. For the photons 1.0×10^8 and for the electrons 5.0×10^7 histories were tracked and the dose deposited in each voxel of the phantoms in cGy was determined.

Calculation

Photon SAF

The absorbed energy in each organ was calculated as sum of the absorbed energy in the entire voxels of the organ. Mass of the

energy (keV)	target organ	method	source organ					
			liver	kidneys	lungs	pancreas	spleen	adrenals
100	liver	GATE	8.81E-02	2.26E-02	1.35E-02	2.86E-02	5.61E-03	4.31E-02
		MCNP4B	9.01E-02	2.32E-02	1.42E-02	2.89E-02	5.73E-03	4.35E-02
		MCNPX	8.67E-02	2.19E-02	1.29E-02	2.79E-02	5.28E-03	4.21E-02
	kidneys	GATE	2.26E-02	1.64E-01	6.59E-03	4.37E-02	3.53E-02	7.70E-02
		MCNP4B	2.31E-02	1.65E-01	6.82E-03	4.36E-02	3.65E-02	7.65E-02
		MCNPX	2.16E-02	1.62E-01	6.16E-03	4.23E-02	3.43E-02	7.48E-02
	lungs	GATE	1.38E-02	6.70E-03	5.01E-02	1.13E-02	1.64E-02	1.27E-02
		MCNP4B	1.42E-02	6.81E-03	5.02E-02	1.14E-02	1.70E-02	1.27E-02
		MCNPX	1.30E-02	6.22E-03	4.88E-02	1.07E-02	1.56E-02	1.19E-02
	pancreas	GATE	2.88E-02	4.39E-02	1.11E-02	8.21E-01	3.44E-02	1.60E-01
		MCNP4B	2.88E-02	4.35E-02	1.12E-02	8.20E-01	3.54E-02	1.60E-01
		MCNPX	2.85E-02	4.30E-02	1.10E-02	8.15E-01	3.34E-02	1.57E-01
	spleen	GATE	5.53E-03	3.51E-02	1.60E-02	3.39E-02	2.55E-01	2.44E-02
		MCNP4B	5.75E-03	3.62E-02	1.67E-02	3.51E-02	2.59E-01	2.47E-02
		MCNPX	5.25E-03	3.39E-02	1.54E-02	3.28E-02	2.51E-01	2.34E-02
	adrenals	GATE	4.32E-02	7.67E-02	1.27E-02	1.60E-01	2.43E-02	3.35E+00
		MCNP4B	4.31E-02	7.57E-02	1.30E-02	1.63E-01	2.33E-02	3.34E+00
		MCNPX	4.05E-02	7.55E-02	1.22E-02	1.59E-01	2.39E-02	3.31E+00
200	liver	GATE	8.39E-02	2.02E-02	1.23E-02	2.50E-02	5.25E-03	3.80E-02
		MCNP4B	8.63E-02	2.10E-02	1.51E-02	2.57E-02	5.55E-03	3.89E-02
	kidneys	GATE	2.02E-02	1.64E-01	6.18E-03	3.92E-02	3.20E-02	7.18E-02
		MCNP4B	2.10E-02	1.67E-01	7.07E-03	3.98E-02	3.32E-02	7.27E-02
	lungs	GATE	1.24E-02	6.19E-03	4.88E-02	9.96E-03	1.48E-02	1.12E-02
		MCNP4B	1.29E-02	6.53E-03	4.37E-02	1.03E-02	1.56E-02	1.15E-02
	pancreas	GATE	2.52E-02	3.93E-02	9.95E-03	8.58E-01	2.96E-02	1.52E-01
		MCNP4B	2.54E-02	3.94E-02	1.17E-02	8.67E-01	3.08E-02	1.54E-01
	spleen	GATE	5.20E-03	3.19E-02	1.47E-02	2.94E-02	2.55E-01	2.17E-02
		MCNP4B	5.47E-03	3.31E-02	1.93E-02	3.06E-02	2.61E-01	2.24E-02
	adrenals	GATE	3.85E-02	7.18E-02	1.13E-02	1.52E-01	2.18E-02	3.70E+00
		MCNP4B	3.96E-02	7.25E-02	1.10E-02	1.54E-01	2.32E-02	3.74E+00

Tab. 2 SAF values (kg^{-1}) for 100–1000 keV photons derived with GATE4.0.0, MCNP4B (data derived from ref. 34, 40) and MCNPX (11) using Zubal phantom

organ was calculated by summing up the density of the voxels belonging to the respective organ multiplied by the voxel volume (4×4×4 mm).

Based on the MIRD schema (27), specific absorbed fraction (SAF) was calculated as the fraction of the emitted energy from the source organ (r_s) that is absorbed in the target organ (r_t) per unit mass of the target organ (27):

$$SAF(r_t \xleftarrow{E} r_s) = \frac{\text{energy adsorbed in } r_t \,/\, \text{energy emitted from } r_s}{m} \quad (1)$$

SAF is independent of the radionuclide half-life and is used to estimate the mean absorbed dose for the different radionuclides in practice (9, 18). The photon SAFs estimated in this study were based on the Zubal adult voxel phantom and are only valid for this condition.

Electron S-factor

S-factor is defined as the product of emitted energy per disintegration and the absorbed fraction for a given combination of a source and a target regions and for the type of radiation emitted divided by the mass of the target region (19). S-factor therefore, is strongly dependent on the geometry of both the source and the target re-

Tab. 2
Continued

energy (keV)	target organ	method	source organ					
			liver	kidneys	lungs	pancreas	spleen	adrenals
500	liver	GATE	8.34E-02	1.89E-02	1.16E-02	2.31E-02	4.97E-03	3.54E-02
		MCNP4B	8.41E-02	1.93E-02	1.40E-02	2.34E-02	5.15E-03	3.57E-02
		MCNPX	8.30E-02	1.88E-02	1.15E-02	2.29E-02	4.93E-03	3.53E-02
	kidneys	GATE	1.90E-02	1.68E-01	5.86E-03	3.67E-02	3.06E-02	6.98E-02
		MCNP4B	1.95E-02	1.68E-01	6.63E-03	3.71E-02	3.10E-02	7.01E-02
		MCNPX	1.89E-02	1.67E-01	5.81E-03	3.64E-02	3.05E-02	6.94E-02
	lungs	GATE	1.16E-02	5.85E-03	4.84E-02	9.07E-03	1.40E-02	1.02E-02
		MCNP4B	1.19E-02	6.06E-03	4.23E-02	9.27E-03	1.43E-02	1.04E-02
		MCNPX	1.15E-02	5.88E-03	4.84E-02	9.07E-03	1.40E-02	1.02E-02
	pancreas	GATE	2.31E-02	3.68E-02	9.12E-03	9.00E-01	2.71E-02	1.50E-01
		MCNP4B	2.34E-02	3.69E-02	1.05E-02	8.97E-01	2.72E-02	1.51E-01
		MCNPX	2.31E-02	3.65E-02	9.15E-03	8.95E-01	2.69E-02	1.49E-01
	spleen	GATE	4.95E-03	3.05E-02	1.40E-02	2.69E-02	2.62E-01	2.01E-02
		MCNP4B	5.19E-03	3.11E-02	1.80E-02	2.76E-02	2.63E-01	2.06E-02
		MCNPX	4.95E-03	3.05E-02	1.39E-02	2.67E-02	2.61E-01	2.00E-02
	adrenals	GATE	3.53E-02	6.99E-02	1.03E-02	1.50E-01	1.97E-02	3.92E+00
		MCNP4B	3.64E-02	6.91E-02	1.32E-02	1.53E-01	1.95E-02	3.90E+00
		MCNPX	3.39E-02	7.12E-02	1.06E-02	1.51E-01	1.97E-02	3.89E+00
1000	liver	GATE	7.59E-02	1.73E-02	1.06E-02	2.09E-02	4.72E-03	3.21E-02
		MCNP4B	7.58E-02	1.74E-02	1.07E-02	2.10E-02	4.82E-03	3.22E-02
	kidneys	GATE	1.74E-02	1.52E-01	5.43E-03	3.33E-02	2.80E-02	6.38E-02
		MCNP4B	1.76E-02	1.51E-01	5.49E-03	3.34E-02	2.82E-02	6.34E-02
	lungs	GATE	1.06E-02	5.45E-03	4.28E-02	8.28E-03	1.27E-02	9.27E-03
		MCNP4B	1.07E-02	5.53E-03	4.25E-02	8.32E-03	1.29E-02	9.35E-03
	pancreas	GATE	2.09E-02	3.33E-02	8.21E-03	8.04E-01	2.44E-02	1.38E-01
		MCNP4B	2.10E-02	3.26E-02	8.18E-03	7.97E-01	2.41E-02	1.37E-01
	spleen	GATE	4.73E-03	2.80E-02	1.27E-02	2.44E-02	2.38E-01	1.83E-02
		MCNP4B	4.82E-03	2.80E-02	1.28E-02	2.46E-02	2.37E-01	1.85E-02
	adrenals	GATE	3.21E-02	6.41E-02	9.11E-03	1.36E-01	1.85E-02	3.26E+00
		MCNP4B	3.31E-02	6.22E-02	9.45E-03	1.38E-01	1.82E-02	3.20E+00

gions and on the quality of the emitted radiation.

Conceptually SAF and S-factor are similar; however, the S-factor has a unit of mGy/MBq-s that is more comprehensive in clinical applications. In theory, the relation between the two is given by: $S = \Sigma i\, \Delta i \times SAF$, where Δi is the mean energy of the i^{th} transition per nuclear transformation of a specific isotope (5). Since we are comparing results from monoenergetic particles, the relation reduces to $S = E \times SAF$, where E is the energy of the particle in question. We have chosen to present our results using quantities that were used by Yoriyazet al. and Stabin et al. (34, 40) i. e.: SAF for photon comparison and S-factor for electron comparison.

Data analysis

The relative percentage difference (RD%) between two corresponding photon SAF values was calculated as;

$$RD\,\% = 100 \times [SAF_{GATE} - SAF_{MCNP}] / [(SAF_{GATE} + SAF_{MCNP})/2] \quad (2)$$

Tab. 3 Comparison between the photon SAF values derived with GATE/GEANT and MCNP4B Monte Carlo Packages

photon energy (keV)	correlation		agreement bias (%)	maximum relative difference	
	linear curve equation	r^2		RD (%)	target ← source
10	$SAF_{GATE} = 1.016 \times SAF_{MCNP4B}$	0.999	–6.8	21	pancreas ← liver
15	$1.026 \times SAF_{MCNP4B}$	0.709	–11.4	53	liver ← spleen
20	$1.010 \times SAF_{MCNP4B}$	0.999	–2.7	25	adrenals ← spleen
30	$1.002 \times SAF_{MCNP4B}$	0.999	0.7	16	adrenals ← adrenals
50	$0.994 \times SAF_{MCNP4B}$	0.999	2.5	11	adrenals ← adrenals
100	$1.004 \times SAF_{MCNP4B}$	0.999	–1.3	05	liver ← lungs
200	$1.012 \times SAF_{MCNP4B}$	0.998	–4.1	26	spleen ← lungs
500	$1.011 \times SAF_{MCNP4B}$	0.997	–3.3	25	spleen ← lungs
1000	$1.001 \times SAF_{MCNP4B}$	0.999	–0.3	04	adrenals ← lungs
100[a]	$SAF_{MCBPX} = 0.985 \times SAF_{MCNP4B}$	0.999	–4.5	10	kidneys ← lungs
500[a]	$SAF_{MCNPX} = 0.987 \times SAF_{MCNP4B}$	0.997	–3.7	25	spleen ← lungs

[a] comparison of SAF values derived MCNPX and MCNP4B

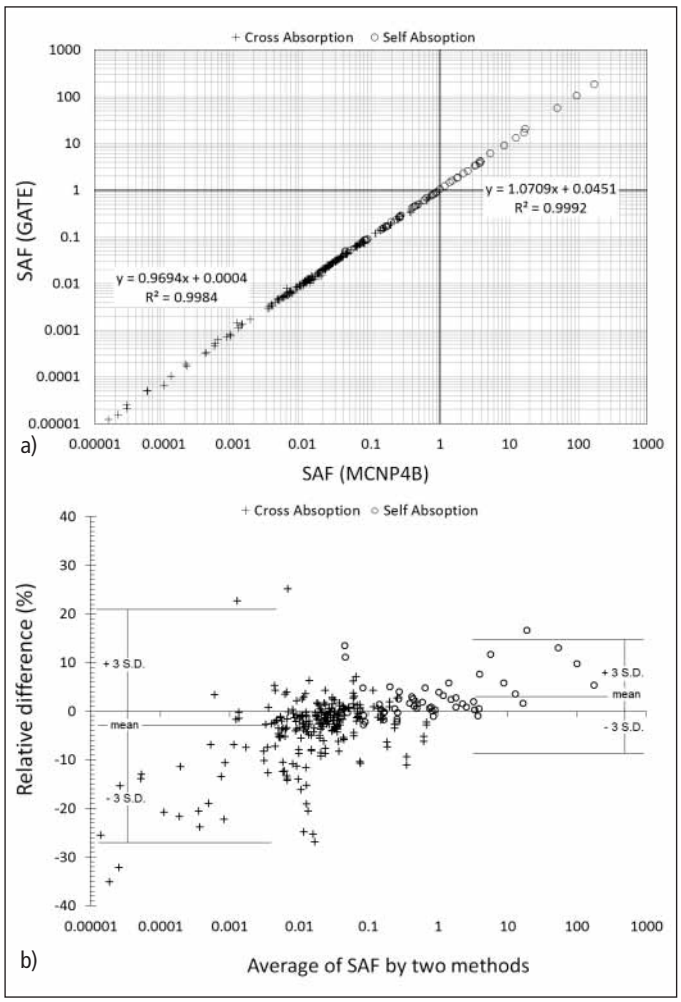

Fig. 1 The whole data from the GATE/GEANT and MCNP4B were divided into two groups, cross-irradiation, and self-absorption. **a)** Linear curves were fitted to the data and Pearson's correlation coefficients were calculated. The graphs are shown in logarithmic scale. **b)** Bland-Altman analysis of the data showed negative and positive biases for cross-irradiation and self-absorption, respectively.

Since we do not know which of the corresponding photon SAF values (GEAT/GEANT or MCNP4B) are correct, the average values were considered for the calculation of relative percentage differences (40). One-sample Kolmogorov-Smirnov test (MATLAB statistics toolbox, version 7.1) was used to test if RD% values are normally distributed around their mean. Bland-Altman analysis (28) was used to determine agreement and bias between the data derived with GATE/GEANT and MCNP4B. Paired t-test was used to compare the mean values of the photon SAFs derived with GATE/GEANT and MCNP4B.

Results

Comparisons derived with GATE/GEANT and MCNP4B

Photon SAF

The *SAF* values (six combinations of the source and target organs) derived for the photons of 10, 15, 20, 30, 50, 100, 200, 500 and 1000 keV using GATE/GEANT code are presented in (▶Tab. 1, ▶Tab. 2). The *SAF* values derived using MCNP4B (34, 40) and MCNPX (11) (when available) were also included in the tables for the sake of comparison. The data in each table were analyzed independently and the results are presented row-wise in (▶Tab. 3). The first column of the table represents the energy of the photons, in the next two columns are the equations of the linear curves fitted to the GATE/GEANT and the MCNP4B scatter plot and the corresponding Pearson's correlation coefficients respectively. The forth column represents the Bland-Altman bias between the GATE/GEANT and the MCNP4B data. In the fifth and sixth columns, the maximum relative percentage differences between the GATE/GEANT and MCNP data and corresponding pair of organs($_{target \leftarrow source}$) are presented.

The photon SAF values derived with GATE/GEANT and MCNP4B were pooled and divided into two groups, self-absorption, and cross-irradiation. ▶Figure 1a represents the scatter plot of the data and the linear curves fitted to them. The linear curve

fitted to the self-absorption and cross-absorption data were $SAF_{GATE} = 1.071 \times SAF_{MCNP\ 4B}$ and $SAF_{GATE} = 0.970 \times SAF_{MCNP\ 4B}$, respectively. In both cases, the Pearson's correlation coefficients were high ($r^2 \geq 0.99$) showing very good linear correlation between the two series of data. However, Bland-Altman analysis (▶Fig. 1b) showed a bias between the GATE/GEANT and MCNP4B results. The SAF values derived with the GATE/GEANT for the self-absorption was +2.7% higher and for the cross-irradiation was –2.9% smaller than corresponding SAF values derived with the MCNP4B (40). This suggest a systematic rather than statistical random difference between the GATE/GEANT and the MCNP4B results. One-sample Kolmogorov-Smirnov test rejected that the relative percentage differences in the SAF values (Eq-2) are normally distributed around their mean. Analyzing the histogram of the RD% values for the self-absorptions and the cross-irradiation suggested that the bias between the GATE/GEANT and the MCNP4B results are likely due to outlier data.

In ▶Figure 2a, the SAF values against the photon energy are presented for the self-absorption data. The graphs visually reveal a good correlation between the two series of data however, with minimum 3 to maximum 17% higher values for GATE/GEANT compared to MCNP4B. In ▶Figure 2b, the SAF values for the spleen (as source) to other organs (targets) against photon energies are presented. The graphs show good correlation between the two series of data but smaller values for GATE/GEANT compared to MCNP4B. In ▶Figure 2c the SAF values for the lungs as source organ against the photon energies are presented. The graphs reveal similar results that is, a good correlation between the two series of data but smaller values for GATE/GEANT. However, for the photons of 200 and 500 keV, the SAF values derived using MCNP4B were exceptionally higher than the corresponding value derived using GATE/GEANT, revealing second peaks in the lungs cross-irradiation curves.

In ▶Figure 3 the average relative percentage differences against photon energy are plotted. As can be seen the average percentage differences do not obey a physically explainable trend. For almost all the photon energies, the self-absorption is higher (except for the 100 keV photons) and the cross-irradiation is lower (except for the 50 keV photons) in the GATE/GEANT results compared to the MCNP4B. ▶Table 3 reveals that the maximum and the minimum differences between the GATE/GEANT and MCNP4B results are with the photon energy of 15 keV and 1000 keV respectively. The absolute relative difference between the GATE/GEANT and MCNP4B results for the photon of 15 (▶Tab. 1) and 1000 keV (▶Tab. 2) are presented graphically in ▶Figure 4a and 4b. In organ-wise comparison, the photon SAF values for ($_{adrenals \leftarrow adrenals}$) and ($_{spleen \leftarrow lungs}$) showed the maximum

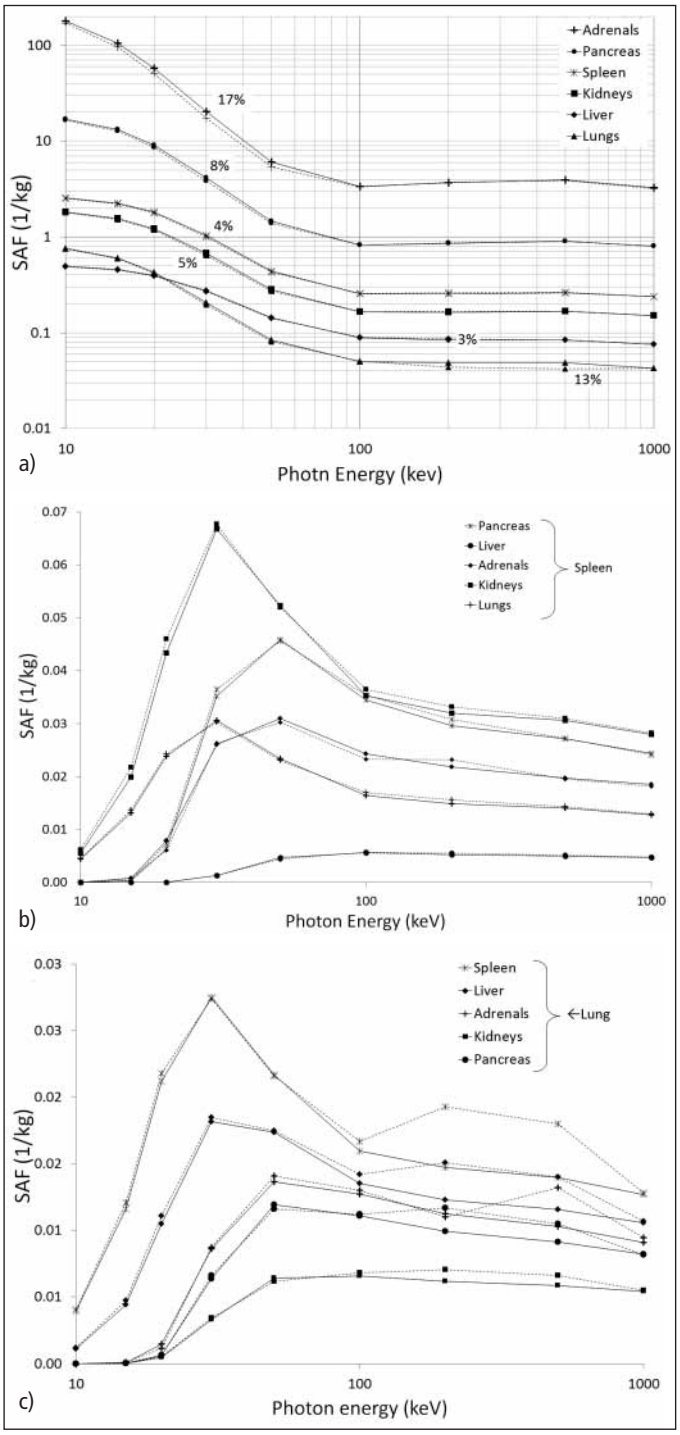

Fig. 2
Photon SAF values derived with the GATE/GEANT (solid line) and MCNP4B (dashed line) against the photon energy:
a) Self-absorption of all the organs investigated, the maximum of difference over each curve is labeled.
b) Cross-irradiation from the spleen to other organs investigated.
c) Cross-absorption from lungs to other organs. It is clear that MCNP4B deviates from GATE/GEANT at photon energies of 200 and 500 keV.

relative difference between the GATE/GEANT and MCNP results.

In comparison of the SAF values derived using MCNP4B and MCNPX there were 4.8% and 3.9% positive bias for MCNP4B compared to MCNPX for the photons of 100 keV and 500 keV respectively.

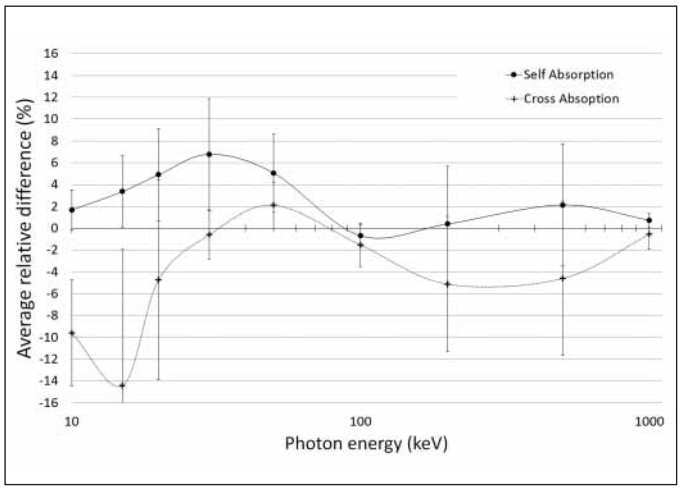

Fig. 3
Average of relative percentage difference between the GATE/GEANT and MCNP4B for self-absorption and cross-irradiation against the photon energy: Exceptionally the difference between the SAF derived with the GATE/GEANT and the MCNP4B results are high (-14.4%) at photon energy of 15 keV.

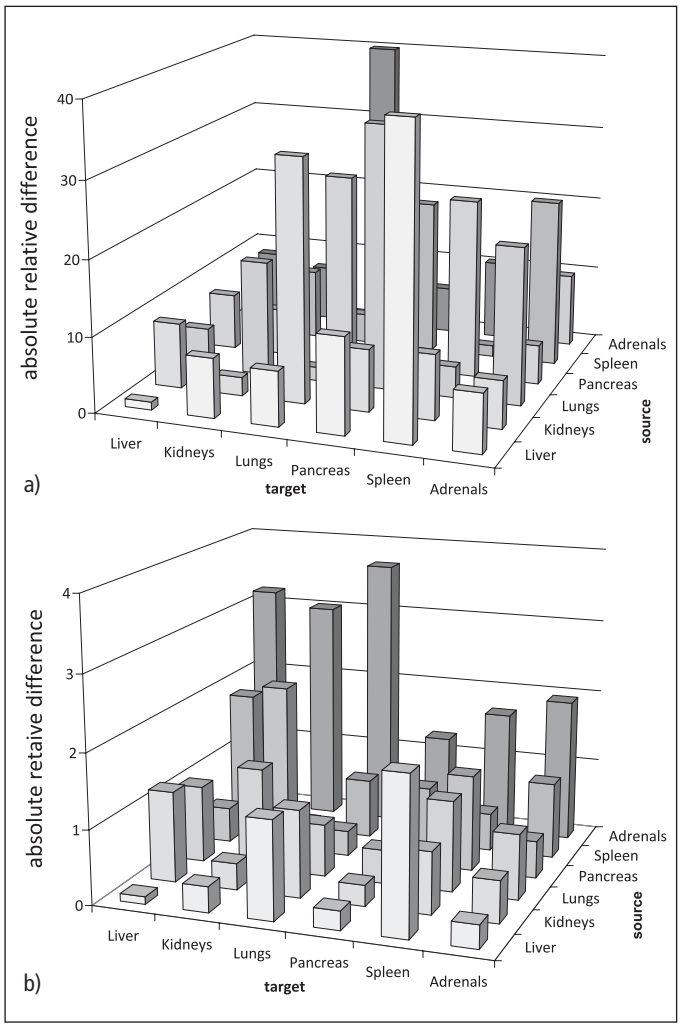

Fig. 4
Absolute relative difference between SAF derived with GATE/GEANT and MCNP4B for photon energy of 15 keV (a) and 100 keV (b): The relative difference is almost 10 times more for 15 keV photons. This cannot simply be interpreted as random error. Some of the data bars are hidden by others however this is the optimized 3D views of the graph.

Electron S-factors

We calculated the S-factors for the electron-emitting source (935 keV) uniformly distributed in the liver, kidneys, and lungs (Zubal phantom) and the results are presented in ▶Table 4. For the sake of comparison, similar data published by Yoriyaz et al (derived using MCNP4B) and Chiavassa et al (derived using MCNPX) are included in the table. There was a good correlation between the GATE/GEANT and the MCNP4b results ($S_{GATE} = 0.994 \times S_{MCNP\ 4B}$, $r^2 = 0.999$) almost at the same level as between the MCNP4B and the MCNPX results ($S_{MCNP\ 4B} = 0.996 \times S_{MCNPX}$, $r^2 = 0.999$). The relative percentage difference between the S-factors derived using GATE/GEANT, MCNP4B and MCNPX are shown in ▶Figure 5. The maximum relative difference observed was between MCNPX and MCNP4B for ($_{kidneys \leftarrow lungs}$). Bland-Altman analysis showed a positive bias of +3.5% for the S-factors derived using MCNP4B compared to MCNPX.

Discussion

The aim of present study was to compare GATE/GEANT with the older and well-developed Monte Carlo code constituting a validation of GATE/GEANT for internal dosimetry using anthropomorphic voxel phantom. Two publications could be used for this comparison. Yoriyaz et al. and Stabin et al. (34, 40) published SAFs for mono-energetic photons of 10 keV to 4 MeV and S-factors for mono-energetic electrons of 935 keV using the MCNP4B code and the Zubal phantom. Chiavassa et al. (11) also provided SAFs for mono-energetic photons of 100 and 500 keV and S-factors for mono-energetic electrons of 935 keV using MCNPX code and Zubal phantom.

Effectively, there is no statistical test available for this type of comparison. Thus, different tests were used to compare the data from different points of view. In the first step, we divided the photon SAF values into two groups, the self-absorption and the cross-irradiation. Pearson's correlation coefficients showed very good linear correlation between the GATE/GEANT and MCNP4B results in both groups. However,

Bland-Altman analysis showed +2.7% and –2.9% bias for the self-absorption and the cross-irradiation respectively. Paired t-test proved that the difference in the self-absorption group was statistically significant ($p > 0.24$) but failed to prove the significance of difference in the cross-irradiation group ($p < 0.01$). The failure was most probably due to higher statistical variation in cross-absorption data compared to self-absorption data (▶Fig. 1b). Therefore, the difference between the GATE/GEANT and MCNP4B results are not just due to statistical variation and something must be different between our simulation and those of Yoriyaz et al and Stabin et al. (34, 40).

Damet et al., in studying the response of thyroid monitors to anatomical variation, compared GEANT4 (the base of GATE) and MCNP5 in an anthropomorphic phantom (GEDI) and reported 2% higher values for GEANT4 (13). They simulated the detector response to ^{131}I radiation and related the difference to details of the decay scheme considered in the codes. Since the main advantage of GATE over GEANT4 is voxelization and ease of use; the physics is in principle the same, in present study mono-energetic photons and electrons were considered in GATE. Pacilio et al., compared GEANT4 and MCNP and reported up to 10% difference in voxel S-factors. However, in present study the dose to the organs were considered not to the voxels. The difference in voxels may be canceled when the values are summed up to calculated the dose to the organs (30).

A simple explanation for the observed difference between GATE/GEANT and MCNP4B may be higher attenuation properties of the tissues in our study compared to the Yoriyaz et al. and Stabin et al. (34, 40). Difference in attenuation properties would certainly result in higher absorption in source organs and therefore lowers cross-irradiation to target organs. However, we used exactly the same geometry as used by Yoriyaz et al. and Stabin et al.

▶Figure 3 clearly shows that the bias between the GATE/GEANT and MCNP results exist at all photon energies and does not follow a physically explainable trend. Hence, the bias is almost independent of the photon energy. If the tissue attenuation properties were different between our and the references studies, the relative differences would reduce by increasing the photon energy. This means that the differences are not related to the difference in the average molecular weight or the material composition attributed to the tissues. The tissue compositions were not explicitly given in the reference studies (34, 40); the tissue compositions for the present study were those supplied by the GATE software.

Although ▶Figure 4 shows that the absolute relative difference between GATE/GEANT and MCNP4B for the photons of 15 keV is almost 10 times higher than the photons of 1000 keV. However, it does suggest dependency of the relative differences to the photon energy. Low energy photons (e. g. 15 keV) have very low penetration (from source to target) and therefore corresponding SAF values are very small in magnitude. Statistically, uncertainty is inversely proportional to absolute value of data. Therefore, this difference was most likely due to high statistical uncertainty in data derived for the photon energy of 15 keV.

▶Figure 2c shows that lung SAF values derived using MCNP4B have a second peak between 200 and 500 keV photons. As can be seen the photon SAF values derived using GATE/GEANT are monotonically descending in this range of energy, which is theoretically expected. This suggests an inconsistency in between MCNP4B results. To some extent, the observed difference between the GATE/GEANT and MCNP4B results was due to inconsistency in MCNP4B results.

A close look at ▶Figure 4 reveals that the relative percentage differences are different in different organs. On average, the relative percentage differences were higher

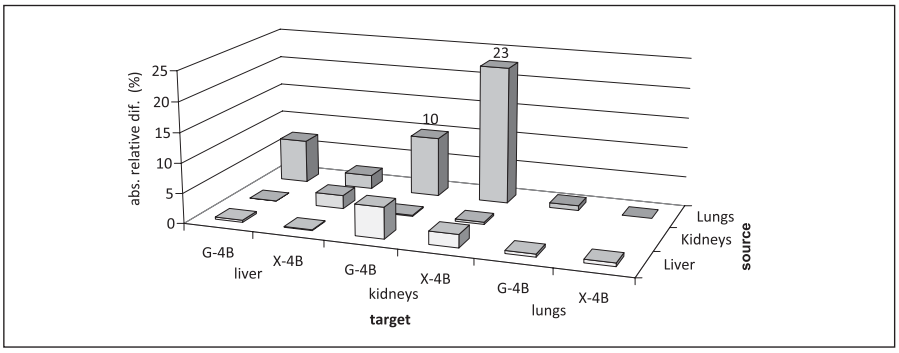

Fig. 5 Absolute relative percentage difference between the S-factors derived with the GATE-MCNP4B (G-4B) and MCNPX-MCNP4B (X-4B): The difference between GATE/GEANT and MCNP4B is below 5% except for the lungs. As can be seen the difference between MCNP4B and MCNPX is very high.

Tab. 4 Electron S-factors (mGy Mbq^{-1} s^{-1}) for 935 keV electrons derived with GATE, MCNP4B using Zubal phantom

target organ	method	source organ		
		liver	kidneys	lungs
liver	GATE	7.38E-05	4.42E-07	1.64E-07
	MCNP4B	7.35E-05	4.42E-07	1.76E-07
	MCNPX	7.36E-05	4.52E-07	1.72E-07
kidneys	GATE	4.41E-07	2.72E-04	3.52E-09
	MCNP4B	4.65E-07	2.72E-04	3.17E-09
	MCNPX	4.55E-07	2.71E-04	2.52E-09
lungs	GATE	1.74E-07	4.17E-09	1.13E-04
	MCNP4B	1.73E-07	0.00E+00	1.12E-04
	MCNPX	1.74E-07	2.52E-09	1.12E-04

data derived from [a](34, 40) and [b](11)

in the paired organs (5.53±6.95%) compared to single organs (4.42±6.40%). Due to high standard deviations the difference was not statistically significant ($p < 0.05$), the absolute difference was high enough that demands an explanation. A feasible explanation for this observation is the cross firing between the paired organs. The absorbed dose in paired organs is composed of two components, the self-absorption and the dose due to cross firing from the counterpart organ. This results in over estimation of self-absorption and consequently lower estimation of cross-irradiation. We did not correct this effect and treated paired organs (kidneys, lungs and adrenal glands) just like single organs (liver, spleen and pancreas) in calculation of photon SAF values. It is not clear whether this effect was considered in the calculation of photon SAFs in the reference paper used in this study (34, 40).

In ▶ Figure 5, the absolute relative differences between S-factors derived using GATE/GEANT and MCNP4B are presented. Except with the lungs, the differences observed with other organs are below 5%, showing good linear correlation between the GATE/GEANT and MCNP4B results. However, the relative percentage differences between the S-factors derived using GATE/GEANT and MCNP4B for the cross-absorption of lungs to kidneys was 10%. The corresponding difference between MCNP4B and MCNPX was 23%. These differences were probably due to high statistical uncertainty in absolute value of photon SAF. The SAFs for cross-irradiation of lungs to kidneys were in order of 10^{-9}.

Analyzing data in ▶ Table 4, showed that the relative percentage difference between the MCNPX and the MCNP4B codes that are two versions of the same package was almost at the same level as between the GATE/GEANT and MCNP, with +3.5% bias for MCNP4B compared to MCNPX. Chiavassa et al. (11) reported up to 23% differences between MCNP4B and MCNPX for electron cross-irradiation. Since S-factors for cross-irradiation of electrons were small in magnitude, at least to some extent the differences were a reflection of statistical variation however, the table of cross-sections are different in MCNP4B and MCNPX (29).

Conclusion

There was a very good linear correlation between the photon SAF values and electron S-factors derived using GATE/GEANT and MCNP4B. However, there was a bias between the two series of data:

- GATE/GEANT produced higher SAF values for self-absorption, but lower values for cross-irradiation.
- The differences were organ dependent and higher for paired organs compared to single organs.

The differences, to some extent, were depended upon the absolute value of data. When the absolute values of photon SAF and electron S-factors were small the agreement between the two series of data was weak. Irrespective to this explanation the table of cross-section used in two codes are different. However, difference at this level is acceptable and we can conclude that GATE/GEANT produces almost similar results as MCNP4B.

Acknowledgement

The work underlying this paper was supported by a grant from Tarbiat Modares University.

Conflict of interest

The authors declare, that they have no conflict of interest.

References

1. Andreo P. Monte Carlo techniques in medical radiation physics. Phys Med Biol 1991; 36: 861–920.
2. Assié K, Gardin I, Véra P, Buvat I. Validation of the Monte Carlo simulator GATE for indium-111 imaging. Phys Med Biol 2005; 50: 3113–3125.
3. Bentourkia M, Sarrhini O. Simultaneous attenuation and scatter corrections in small animal PET imaging. Comput Med Imaging Graph 2009; 33: 477–488.
4. Bland JM, Altman DG. Statistical methods for assessing agreement between two methods of clinical measurement. Int J Nurs Stud 2010; 47: 931–936.
5. Bolch WE, Eckerman KF, Sgouros G, Thomas SR. MIRD pamphlet No. 21: a generalized schema for radiopharmaceutical dosimetry--standardization of nomenclature. J Nucl Med 2009; 50: 477–484.
6. Briesmeister JF. MCNP–A General Monte Carlo N–Particle Transport Code Version 4C. Los Alamos National Laboratory Report 2000.
7. Buvat I, Castiglioni I. Monte Carlo methods in PET and SPECT. Q J Nucl Med 2002; 46: 48–59.
8. Carrier JF, Archambault L, Beaulieu L, Roy R. Validation of GEANT4, an object-oriented Monte Carlo toolkit, for simulations in medical physics. Med Phys 2004; 31: 484–492.
9. Chao TC, Xu' XG. Specific absorbed fractions from the image-based VIP-Man body model and EGS4-VLSI Monte Carlo code: internal electron emitters. Phys Med Biol 2001; 46: 901–927.
10. Charles WS, Schmidtlein CS, Kirov AS et al. Validation of GATE Monte Carlo simulations of the GE Advance/Discovery LS PET scanners. Med Phys 2006; 33: 198–208.
11. Chiavassa S, Aubineau-Laniece I, Bitar A et al. Validation of a personalized dosimetric evaluation tool (Oedipe) for targeted dradiotherapy based on the Monte Carlo MCNPX code. Phys Med Biol 2006; 51: 601–616.
12. Chiavassa S, Manuel B, Françoise G-V et al. OEDIPE: A Personalized Dosimetric Tool Associating Voxel-Based Models with MCNPX. Cancer Biother Radiopharm 2005; 20: 325–332.
13. Damet J, Bochud FO, Bailat C et al. Variability of radioiodine measurements in the thyroid. Radiat Prot Dosimetry 2010; doi:10.1093/rpd/ncq312.
14. Flux G, Bardies M, Monsieurs M et al. The impact of PET and SPECT on dosimetry for targeted radionuclide therapy. Z Med Phys 2006; 16: 47–59.
15. Geworski L, Schaefer A, Knoop B et al. Physical aspects of scintigraphy-based dosimetry for nuclear medicine therapy. Nuklearmedizin 2010; 49: 85–95.
16. Glatting G, Landmann M, Wunderlich A et al. Internal radionuclide therapy: Software for treatment planning using tomographic data. Nuklearmedizin 2006; 45: 269–272.
17. Guimarães CC, Moralles M, Okuno E. Performance of GEANT4 in dosimetry applications: Calculation of X-ray spectra and kerma-to-dose equivalent conversion coefficients. Radiat Meas 2008; 43: 1525–1531.
18. Hakimabad HM, Motavalli LR. Evaluation of specific absorbed fractions from internal photon sources in ORNL analytical adult phantom. Radiat Prot Dosimetry 2008; 128: 427–431.
19. Hindorf C, Ljungberg M, Strand S-E. Evaluation of parameters influencing S values in mouse dosimetry. J Nucl Med 2004; 45: 1960–1965.
20. Hobbs RF, Wahl RL, Lodge MA et al. ^{124}I PET-based 3D-RD dosimetry for a pediatric thyroid cancer patient: Real-time treatment planning and methodologic comparison. J Nucl Med 2009; 50: 1844–1847.
21. Jan S, Santin G, Strul D et al. GATE:a simulation toolkit for PET and SPECT. Phys Med Biol 2004; 49: 4543–4561.
22. Jiang H, Paganetti H. Adaptation of GEANT4 to Monte Carlo dose calculations based on CT data. Med Phys 2004; 31: 2811–2818.
23. Kawrakow I, Rogers DWO. The EGSnrc Code System: Monte Carlo simulation of electron and photon transport: Ionizing Radiation Standards National Research Council of Canada 2000. Report No. NRCC PIRS-701.
24. Kolbert KS, Sgouros G, Scott AM et al. Implementation and evaluation of patient-specific three-dimensional internal dosimetry. J Nucl Med 1997; 38: 301–308.
25. Kron T, Duggay L, Smithk T et al. Dose response of various radiation detectors to synchrotron radiation. Phys Med Biol 1998; 43: 3235–3259.

26. Lazaro D, Bitar ZE, Breton V et al. Fully 3D Monte Carlo reconstruction in SPECT: a feasibility study. Phys Med Biol 2005; 50: 3739–3754.
27. Loevinger R, Budinger TF, Watson EE. MIRD primer for absorbed dose calculations. New York, NY: Society of Nuclear Medicine 1988.
28. Ludovic F, Nicolas C, Abdalkader B et al. Implementing dosimetry in GATE: Dose-point kernel validation with GEANT4 4.8.1. Cancer Biother Radiopharm 2007; 22: 125–129.
29. MCNPX, Version 2.4.0. Los Alamos National Laboratory: LA-UR-02–5253; 2002.
30. Pacilio M, Lanconelli N, Lo M et al. Differences among Monte Carlo codes in the calculations of voxel S values for radionuclide targeted therapy and analysis of their impact on absorbed dose evaluations. Med Phys 2009; 36: 1543–1552.
31. Rodrigues P, Trindade A, Peralta L et al. Application of GEANT4 radiation transport toolkit to dose calculations in anthropomorphic phantoms. Appl Radiat Isot 2004; 61: 1451–1461.
32. Rogers DWO, Mohan R. Questions for comparison of clinical Monte Carlo codes. In: Schlegel W, Bortfeld T (eds). The Use of Comput Radiother; XIIIth Int'l Conf. Heidelberg: Springer 2000: 120–122.
33. Santin G, Staelens S, Taschereau R et al. Evolution of the GATE project: new results and developments. Nucl Phys B (Proc Suppl) 2007; 172: 101–103.
34. Stabin MG, Yoriyaz H. Photon specific absorbed fractions calculated in the trunk of an adult male voxel-based phantom. Health Phys 2002; 82: 21–44.
35. Stabin MG. Uncertainties in internal dose calculations for radiopharmaceuticals. J Nucl Med 2008; 49: 853–860.
36. Staelens S, Strul D, Santin G et al. Monte Carlo simulations of a scintillation camera using GATE: validation and application modelling. Phys Med Biol 2003; 48: 3021–3042.
37. Steven S, de Wit T, Beekman F. Fast hybrid SPECT simulation including efficient septal penetration modelling (SP-PSF). Phys Med Biol 2007; 52: 3027–3043.
38. Taschereau R, Chatziioannou AF (eds). FDG-PET image-based dose distribution in a realistic mouse phantom from Monte Carlo simulations. IEEE Nucl Sci Symp (Conf Rec) 2005, 23–29 Oct.
39. Visvikis D, Bardies M, Chiavassa S et al. Use of the GATE Monte Carlo package for dosimetry applications. Nucl Instrum Meth A 2006; 569: 335–340.
40. Yoriyaz H, dos Santos A, Stabin MG, Cabezas R. Absorbed fractions in a voxel-based phantom calculated with the MCNP-4B code. Med Phys 2000; 27: 1555–1562.
41. Yoriyaz H, Moralles M, Siqueira Pde T et al. Physical models, cross sections, and numerical approximations used in MCNP and GEANT4 Monte Carlo codes for photon and electron absorbed fraction calculation. Med Phys 2009; 36: 5198–5213.
42. Zubal I, Harrell CR, Smith EO et al. Computerized three-dimensional segmented human anatomy. Med Phys 1994; 21: 299–302.